Registration of a Laser Beam Scattered from an Aerosol Located in the Probe Beam Aperture

Vyacheslav F. Myshkin[1,a)], Valeriy A. Khan[1,2,b)], Milan Tichy[3,c)],
Anna Kapran[3,d)], Valentin A. Borisov[1,e)], Denis L. Gamov[1f)]
and Ilya Ju. Zaguzin[1,g)]

[1]*Tomsk Polytechnic University, 634050, Tomsk, Lenina av., 30, Russia*
[2]*V.E. Zuev Institute of Atmospheric Optics SB RAS, 634055, Tomsk, Akademicheski av., 1, Russia*
[3]*Charles University, Faculty of Mathematics and Physics, Ke Karlovu 3, 12116 Praha 2, Czech Republic*

a) Corresponding author: gos100@tpu.ru
b) nt.centre@mail.ru
c) milan.tichy@mff.cuni.cz
d) kapran_anna@mail.ru
e) znk@tpu.ru
f) gdl@tpu.ru
g) ilyatomsk70@yandex.ru

Abstract. An experimental setup has been developed that allows recording the flux of probing radiation scattered from dispersed particles in the 0° direction. To suppress the beam passing through the swarm of dispersed particles a reference beam was used. The reference beam was formed from the probe beam and aligned in the registration plane with the beam passing through the swarm of particles. The Michelson interferometer was tested in an experimental setup to determine the sizes of dust particles of heterogeneous systems. It was shown that by placing a heterogeneous system in one of the arms of the interferometer, it was possible to register the scattered radiation at the angle 0°. This facilitates calculation of the sizes of particles with the same accuracy over the entire size range. To verify the method the iron powder particles sized 50-63 µm were used.

INTRODUCTION

Examples of the heterogeneous systems are found in many natural processes, e.g. in the formation of clouds, as well in the processes created or used by humans, e.g. in the plasma-chemical technologies or in the chemical reactions accompanied by the formation of insoluble compounds. Often, the rate of change in the size of dust particles determines the efficiency of technological processes [1-3]. The formation of dispersed particles is also essential in the separation of carbon isotopes in the process of plasma oxidation of carbon in a magnetic field [4, 5]. The possibility to determine or control the size of dust particles is therefore an important issue for a particular technological process. Dust particles change their size in the low-temperature plasma. In the course of plasma diagnostics, the accumulation of the dust particles on a cold substrate may result in a distortion of the proceeding physical and chemical processes. Consequently, when measuring the size of dust particles in low-temperature plasma, it is beneficial to use non-contact methods [6, 7]. Laser sensing and methods for recording the enlarged images of dust particles do not require accumulating of powder particles on a substrate.

There are several laser diagnostic methods applicable for different dust particle sizes [8, 9]: (i) the spectral transparency method is applicable when $d << \lambda$, (ii) the full indicatrix scattering method can be utilized if $d \approx \lambda$ and (iii) the low-angle scattering method is useful provided that $d >> \lambda$. Here we denoted by d the size of dispersed particles and by λ the wavelength of the probing radiation. The mathematical basis of the laser methods for diagnosing the size distribution of a system of dust particles is the solution of the Fredholm integral equation of the first kind [10] using the experimental data of laser scattering. To calculate the kernel of an integral equation, the Mie theory is used [11, 12].

To determine particle sizes larger than 5 µm, the low-angle scattering indicatrix method is used [13].

However, with an increase in the size of dust particles, the radiation flux scattered at angles close to 0° in the registration plane can be superposed over a collimated beam of radiation that passed through the scattering medium. To minimize this problem, suitable methods are needed to reduce the beam intensity of the probing radiation in the plane of detection of the scattered light.

MATHEMATICAL JUSTIFICATION OF THE METHOD

In order to record the radiation flux scattered in the low-angle region, including the direction of the 0° angle, we have used the interference scheme similar to the one described in [14]. In this system, the beam of collimated laser radiation is divided into two coherent beams: the reference and the probing beams. Further, in the registration plane, the following three beams are spatially superposed: the reference beam, the probing beam passing through the scattering medium without scattering, and the beam of radiation scattered at low angles. Measurement of the scattered radiation intensity at the angle 0° is only possible if the probing beam and the reference laser beam are superposed in the registration plane in the region of one of the interference-minima. The intensity of the probing laser radiation directly passed through the dispersing medium can be reduced below the sensitivity threshold of the matrix photodetector used for that, due to the interference in the scattering indicatrix registration plane. However, only at a certain point the intensity of the total radiation is close to zero owing to the interference. In case of deviation from zero intensity point, the optical path difference deviates from "π" and the intensity of the superposed beam increases; the two beams no longer cancel each other. This limits the range of angles within which it is possible to measure the intensity of the scattered radiation as a function of the wavelength of the probing beam. In the Michelson interferometer, however, the interference fringes are oriented along the probing beam. Therefore, it is possible to reduce the intensity of the coherent superposed beam almost to zero along its entire length. Consider the Michelson interferometer. If the beam-splitting plate divides the light beam into two beams of equal intensities ($I_1 = I_2 = 0.5\ I_0$, where I_0 – the intensity of the probing radiation), then these two waves interact at the output of the interferometer; the corresponding electric field strengths are as follows:

$$E_1 = 2^{-0.5}\ E_0\ \exp[-j(\omega\ t - \varphi_1)], \tag{1}$$
$$E_2 = 2^{-0.5}\ E_0\ \exp[-j(\omega\ t - \varphi_2)]. \tag{2}$$

In these expressions, the symbol φ denotes the phase of the electromagnetic wave.

If the amplitudes of the beams that have passed through different interferometer arms are equal, and there are no losses, then the superposed radiation intensity at the output of the interferometer is given by:

$$I = I_0\ [1 + \cos(\varphi_1 - \varphi_2)]. \tag{3}$$

The signal level at the output of the interferometer depends on the difference of the optical paths of the two beams. The resulting signal can only be set to zero if the lengths of the interferometer arms are accurately balanced and the original beam is divided into two beams of equal intensity.

If an aerosol cloud is located in one of the interferometer arms, then the radiation intensities in the two arms differ from each other. In this case, the superposed radiation intensity in the output plane becomes:

$$I = 0.5\ I_0\ (2 - \alpha) + I_0 \sqrt{1 - \alpha}\ \cos[\varphi_1 - \varphi_2] + 0.5\ I_0\ \sigma_{eff}, \tag{4}$$

where α is the volume attenuation coefficient and σ_{eff} is the volume scattering coefficient in the output aperture of the interferometer.

The intensity of the radiation at the output of the Michelson interferometer, in the measuring arm where the aerosol cloud is located, depends on the following processes: attenuation in the measuring arm of the interferometer, interference of the rays that passed the measuring and reference arms, scattering back into the measuring arm. Formula (4) is obtained by regrouping the members that take into account the contribution of these processes.

If there is just one dust particle in the measuring arm of the interferometer, then the expression (4) is valid for the shadow region. For the radiation intensity outside the shadow area of the dust particle, one can write

$$I = I_0\ (1 + \cos[\varphi_1 - \varphi_2]) + 0.5\ I_0\ \sigma_{eff}. \tag{5}$$

The scattered and the probing beams superpose, and different points along the radius of the reference beam correspond to the beams scattered at different angles. The radiation flux scattered on dust particles diverges while the probing beam is collimated. Therefore, the plane of registration of the scattered radiation must be located close to the beam-splitting plate of the interferometer.

By proper adjustment of the lengths of the interferometer arms for each wavelength it is possible to achieve almost complete attenuation of the intensity of the collimated probing beam behind the interferometer dividing plate ($\Delta L = \lambda / 4$). The scattered beam does not interfere with the probing beam because the scattering process changes the initial plane of polarization. In this case, due to diffraction, the shadow area of the dust particle spreads over the cross section of the probing beam. As a result, the vector subtraction of the intensities of the

two - collimated reference and probing - beams over the entire cross section of their overlap is possible. This allows detection of the scattered radiation at low-angle, including the 0° angle.

EXPERIMENTAL SETUP FOR REGISTRATION OF LOW-ANGLE SCATTERING

To measure the low-angle scattering indicatrix, a Michelson interferometer with the distance between the reflecting mirrors of the interferometer and the beam-splitting plate 20 cm was assembled. In order to cut off the transverse mode components of the LGN-118 laser the output beam was collimated at a distance of 4 m from the laser into a beam of 45 mm in diameter by a telescope. The interferometer was tuned in such a way that the intensity of the output beam after superposition of the radiation of both arms was minimal. An incomplete attenuation of the radiation intensity was observed, however, in some parts of the beam that we attributed to the insufficient quality of the reflecting surface on the beam-splitting plate and the mirrors. A schematic diagram of the experimental set-up for registration of the low-angle scattering indicatrix is shown in Fig. 1.

In the arm of the interferometer, where the powder particles are expected to be placed (the probing arm), we observe the following two probing collimated beams, see Fig. 1: the direct beam that passed through the beam-splitting plate #2 and the same beam reflected from the mirror #4. As a result, when a powder particle is placed into the probing arm, four divergent beams are formed: the scattered and the reflected back diverging beams formed by each of the two probing beams. It is useful to realize, however, that for large particles ($d \gg \lambda$) the intensity of the forward-scattered radiation of the probing beam exceeds by several orders of magnitude the intensity of the reverse-scattered radiation of the same beam [12]. When analyzing the results obtained from experiments with powder particles, we then consider only the intensity of the forward-scattered beam and neglect the reverse-scattered one.
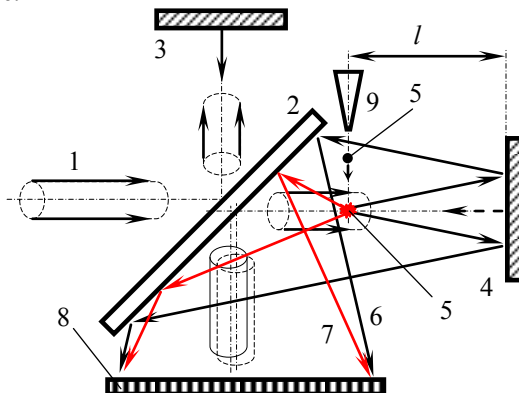

FIGURE 1. Set-up for registration of the low-angle scattering indicatrix: 1 - probing beam, 2 – beam-splitting plate, 3, 4 – mirrors of the reference and the measuring arms of the interferometer, 5 - powder particle, 6, 7 - low-angle and reverse-scattered beams, 8 - CCD matrix, 9 – dispenser

In order to verify the method we placed into the probing arm of the interferometer, into the center of the direct probing beam, the copper winding wire PEV-1, having a diameter with insulation 27 μm. To augment the diffracted radiation intensity of the beam reflected back from the mirror #4 with respect to that of the forward diffracted probing beam, the wire was placed at a distance of 1 cm from the beam-splitting plate of the interferometer.

For registration of the pattern of the diffracted/scattered laser light, we have used the digital camera HS 101H-1024/58 manufactured by the company "SOL instruments Ltd." (http://solinstruments.com/en/). The camera uses a charge-coupled device (CCD) matrix manufactured by Hamamatsu, with 1024×58 pixels sized 24×24 μm oriented horizontally (active area 24.576×1.392 mm). To minimize the thermal noise the CCD matrix is cooled by a Peltier element down to the -20°C. The spectral sensitivity range of the camera is 200-1100 nm. For the data acquisition from the CCD matrix and for visualizing the pattern of the scattered light we have used the PsiLine 4.6.2 software.

The registration plane of the camera was set at a distance of 10 cm from the center of the beam-splitting plate. The camera was installed perpendicular to the beam at the output of the interferometer. Before each measurement series, after letting the CCD to cool down to the operating temperature, the background intensity level of the output beam of the interferometer was recorded. When processing the data the used software automatically subtracted this background level, together with the dark noise of the CCD matrix, from the intensity distribution of the diffracted/scattered radiation.

One of the recorded diffraction patterns of radiation with a wavelength of 632.8 nm (red color) from a wire

with a diameter of 27 μm is shown in Fig. 2; the data accumulation time was 5 seconds. The ordinate axis in Fig. 2 shows the intensity of the recorded radiation in relative units. On the curve in the left panel of Fig. 2 we observe a central maximum and two symmetrical lateral maxima. In the region of the central maximum, we observe an outburst of about 50 relative units and with a width of 0.24 mm (approximately 10 pixels); see the right panel in Fig. 2. That outburst is not seen in the left panel, since its magnitude is insignificant compared to the total amplitude of the scattered radiation intensity of ~12,000 relative units.

The diffracted beams originating from the two probing beams propagate in opposite directions between the beam-splitting plate #3 and the mirror #4 and fall on the photodetector. At the same time, the intensities of these scattered beams are significantly different. Let us estimate the ratio of the intensities of these two scattered beams. The "straight line" distances from the wire to the registration plane were for the direct beam (see the black beam trace in Fig. 1): 19+20+10 = 49 cm, for the beam reflected from the mirror #4 (red trace in Fig. 1): 1+10 = 11 cm. Since the light intensity decays as a square root of the distance, the ratio of the scattered light intensities of the direct beam to that of the beam reflected from the mirror is $(11/49)^2 \cong 0.05$. The scattered light intensity of the beam reflected from the mirror #4 is therefore approximately 20 times higher than that of the direct beam. This shows that by choosing the suitable dimensions of the interferometer and of the position of the "summing volume", i.e. the volume where the superposition of the waves takes place, one can effectively suppress the signal generated by one of the scattered beams on the photo-receiver.
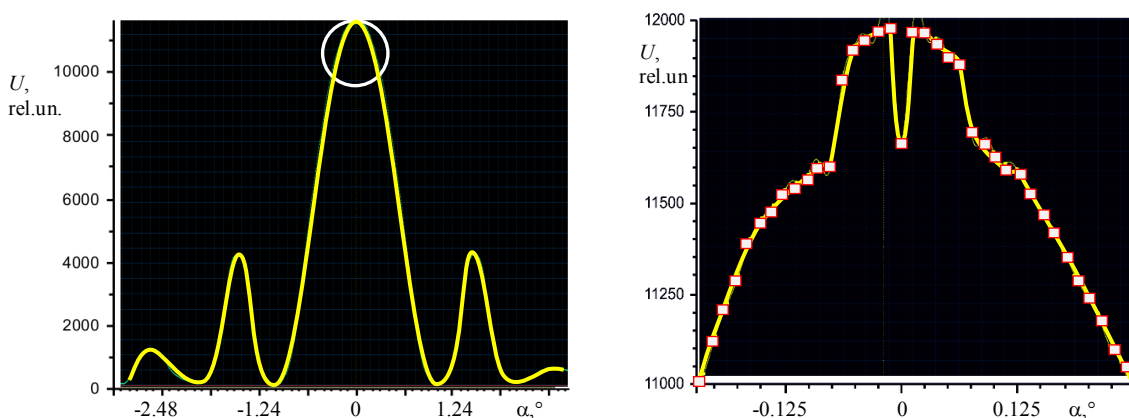

FIGURE 2. Left panel - Diffraction pattern (in dependence on the angle α) recorded by the HS 101H camera. Right panel - Enlarged image of the circled area of the graph on the left

THE EXPERIMENTAL RESULTS

For registering a diffraction pattern on the powder particles we installed a dispenser in the probing arm of the interferometer, which made possible to form a thin stream of powder particles perpendicular to the incident laser beam; the dispenser replaced the wire-fixing unit used in the former experiment. However, the particles leaving the dispenser fly along different trajectories with respect to the probing beam, not just perpendicular to it. Consequently, we had to make provision that the recording device registers also the light scattered on the particles that do not fly exactly perpendicular to the incident beam. To achieve that we have used a thin collecting lens with a focal length of 11 cm; the Fourier transform with the aid of a thin lens does not depend on the location of the object with respect to the optical axis of this lens. We aligned the input focal plane of the lens with the stream of powder, and the output focal plane with the plane of the CCD matrix. As a result, the rays scattered at a certain angle were focused on the same pixel area of the CCD matrix; regardless of the trajectory of powder particles over the cross section of the probing laser beam.

In order to supply the powder particles in a small amount into the probing arm of the interferometer, an air stream flew through a closed volume together with the powder. In such a way, the heterogeneous powder stream was diluted by air resulting in less than 500 powder particles flying across the incident beam per second. The data accumulation time of the CCD camera was set to 5 seconds or more. This ensured the passage of the particles of all sizes through the volume of interaction with light beam during the exposure of the scattering pattern.

When checking the accuracy of the adjustment of the measuring circuit, the following is established. In the "scattering pattern", recorded without the powder particles, a spot with a linear size of 0.168 mm and relative amplitude of 100 units appears. That is a result of the incomplete compensation of the intensities of the probing beams. At the same time, the maximum range of the intensity of the CCD matrix is 12,000 relative units. Consequently, we assessed this "background", coming from the incomplete compensation of the intensities of

the probing beams, as negligible.

The low-angle scattering indicatrix of a helium-neon laser radiation on iron particles, having dimensions in the range of 50-63 μm, is shown in Fig. 3, left panel. The shape of the used powder particles is close to spherical. The assignment of quantities to the axes of the graph is similar as in Fig. 2. In Fig. 3, right panel, we show an enlarged image of the central part of the scattering indicatrix at the angle 0°. The angular distance between the two pixels of the CCD matrix (distanced 25 μm from each other), with a given geometry of the recording stand, is 0.0012°. It can be seen from Fig. 3 that the intensity of the scattered radiation in the range of angles 0°–0.61° changes by more than two orders of magnitude. The character of the scattering indicatrix close to the angle 0° does not show significant changes with respect to the entire low-angle region. There is a burst of intensity in the direction of the probing radiation with a linear size of 1.2 mm on the plane of the CCD matrix, which is significantly larger than the burst size corresponding to the scattering on one powder particle (compare Fig. 2).

The CCD matrix enables recording the scattering indicatrix with the 1024 points resolution. That detailed resolution, however, is redundant when processing the experimental data using an integral equation. Processing matrices with so many columns and rows of the kernel matrix of an integral equation using a PC would require an infinitely long time. In computer processing of indicatrices, we then have used only about 20-25 points selected from the vicinity of the extrema of the scattering indicatrix. The reading of the discrete values of the scattering indicatrix enabled the PsiLine 4.6.2 program used to control the CCD camera.

The experimentally recorded scattering indicatrices of radiation with a wavelength of 632.8 nm were processed on PC using regularizing algorithms [9]. We have based the program that we have used to implement the regularizing algorithm on the patent [14] and the monograph [12, 15] (algorithm and computer program TIKH1). However, when the data of the scattering indicatrix are burdened with higher measuring uncertainty, the solution of the inverse problem diverges - there are many possible solutions that formally satisfy the integral equation. To avoid the problem we used the approach described by us in [16]. In the Table 1 below, we show the data on the relative amount of powder particles of different sizes, which we have obtained after processing one of the experimentally recorded low-angle scattering indicatrix.
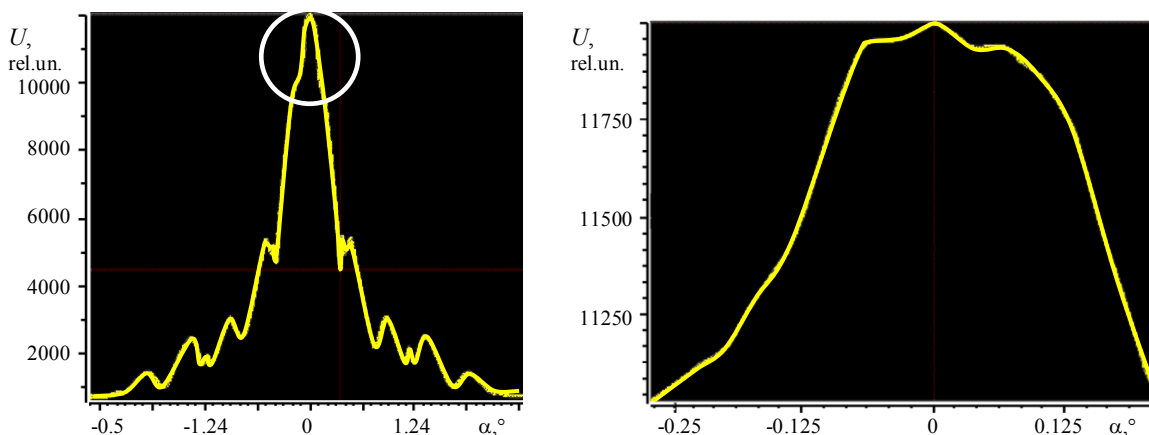

FIGURE 3. Left panel - Small-angle (in dependence on the angle α) scattering indicatrix of red laser light on iron powder particles sized 50-63 μm. Right panel - An enlarged image of the central part of the scattering indicatrix at the angle 0°

TABLE 1. The particle-size statistics of iron-powder particles obtained by processing of the low-angle scattering indicatrix

d, μm	51	53	55	57	59	61	63
n, rel. units	91	122	130	143	127	82	49

The particle-size statistics (Table 1) obtained from the described scattering experiment of the He-Ne laser beam on the iron powder using the Michelson interferometer is in a good agreement with the data obtained from the direct measurements of the particle sizes using an optical microscope.

In order to verify the method we have defined *ex ante* the size distribution function of dust particles and calculated the low-angle scattering indicatrix using the described method. We then processed the calculated scattering indicatrix of the laser radiation from an aerosol with different size distributions. We observed that by processing the low-angle scattering indicatrix of the laser radiation in the visible and near-IR ranges, it was possible to determine the sizes of dust particles in the range of 1–1000 μm. In this size range, the error introduced by the calculation procedures remained almost unchanged if, in the region of the 0° angle, the intensity of the probing radiation did not exceed 14% of the intensity of the scattered radiation.

CONCLUSION

We have shown experimentally that devices, which exploit an interference pattern, such as the Michelson interferometer, permit registration even of a low-angle scattering indicatrix. Such set-ups allow recording the scattered radiation even along the direction of the incident beam, i.e. at the angle 0°. This facilitates the determination of the size of dust particles with almost the same accuracy in the entire size range of 1-1000 μm from the data obtained by laser probing of aerosols.

ACKNOWLEDGMENTS

REFERENCES

1. A. Kotelnikova, A. Karengin and O. Mendoza, AIP Conference Proceedings **1938**, 020015 (2018); doi:10.1063/1.5027222.
2. R. Perekrestov, P. Kudrna, M. Tichý, I. Khalakhan and V. F. Myshkin, Journal of Physics D: Applied Physics **49** (26), 265201 (2016); doi:10.1088/0022-3727/49/26/265201.
3. Yu. Yu. Lutsenko, Technical Physics **50** (11), 1515-1517 (2005); doi:10.1134/1.2131965.
4. Yu. Yu. Lutsenko and E. Lihacheva, AIP Conference Proceedings **1938**, 020008 (2018); doi:10.1063/1.5027215.
5. V. F. Myshkin, E. V. Bespala, V. A. Khan and S. V. Makarevich, IOP Conf. Ser.: Mater. Sci. Eng. **135**, 012029 (2016); doi:10.1088/1757-899X/135/1/012029.
6. G. Ramachandran and D. Leith, Aerosol Science and Technology **17** (4), 303-325 (1992); doi:10.1080/02786829208959578.
7. T. Igushi and H. Yoshida, Review of Scientific Instruments **82**, 015111 (2011); doi:10.1063/1.3520136.
8. V. E. Zuev, V. V. Zuev, B. S. Kostin and E. V. Makienko, Proc. SPIE **1968**, (1993); doi:10.1117/12.154861.
9. A. N. Tikhonov, A. V. Goncharsky, V. V. Stepanov, A. G. Yagola, *Numerical Methods for the Solution of Ill-Posed Problems.* (Kluwer, London, 1995).
10. V.E. Zuev, I.E. Naats, *Inverse Problems of Lidar Sensing of the Atmosphere*, (Springer-Verlag Berlin Heidelberg, 1983), doi:10.1007/978-3-540-38802-9.
11. H.C. Van de Hulst, *Light Scattering by Small Particles* (New York: John Wiley & Sons, 1981).
12. C. F. Bohren and D. R. Huffman, *Absorption and Scattering of Light by Small particles* (New York: Wiley-Interscience, 1998).
13. T. Takagi, J Chromatogr A **506**, 409–416 (1990); doi:10.1016/s0021-9673(01)91596-1
14. V.F. Myshkin, I.A. Tikhomirov, V.N. Tsimbal, The Method of Registration of Low-Angle Indicatrix. Patent RF No.2183828, Bulletin of inventions RF No. 17 (2002). (in Russian).
15. A. F. Verlan and V. S. Sizikov, *Integral Equations: Methods, Algorithms, Programs* (Nauk. Dumka, Kiev, 1986). (in Russian).
16. V. Myshkin, D. Izhoykin, A. Grigoriev, D. Gamov and D. Leontieva, AIP Conference Proceedings **1938**, 020012 (2018); doi:10.1063/1.5027219.